

# Electron Transfer in Nitrogenase Analyzed by Marcus Theory: Evidence for Gating by MgATP<sup>†</sup>

William N. Lanzilotta, Vernon D. Parker, and Lance C. Seefeldt\*

Department of Chemistry and Biochemistry, Utah State University, Logan, Utah 84322

Received July 10, 1997; Revised Manuscript Received October 24, 1997<sup>⊗</sup>

**ABSTRACT:** Nitrogenase-catalyzed substrate reduction reactions require electron transfer between two component proteins, the iron (Fe) protein and the molybdenum–iron (MoFe) protein, in a reaction that is coupled to the hydrolysis of MgATP. In the present work, electron transfer (Marcus) theory has been applied to nitrogenase electron transfer reactions to gain insights into possible roles for MgATP in this reaction. Evidence is presented indicating that an event associated with either MgATP binding or hydrolysis acts to gate electron transfer between the two component proteins. In addition, evidence is presented that the reaction mechanism can be fundamentally changed such that electron transfer becomes rate-limiting by the alteration of a single amino acid within the nitrogenase Fe protein (deletion of Leu 127, L127Δ). These studies utilized the temperature dependence of intercomponent electron transfer within two different nitrogenase complexes: the wild-type nitrogenase complex that requires MgATP for electron transfer and the L127Δ Fe protein–MoFe protein complex that does not require MgATP for electron transfer. It was found that the wild-type nitrogenase electron transfer reaction did not conform to Marcus theory, suggesting that an adiabatic event associated with MgATP interaction precedes electron transfer and is rate-limiting. Application of transition state theory provided activation parameters for this rate-limiting step. In contrast, electron transfer from the L127Δ Fe protein variant to the MoFe protein (which does not require MgATP hydrolysis) was found to be described by Marcus theory, indicating that electron transfer was rate-limiting. Marcus parameters were determined for this reaction with a reorganization energy ( $\lambda$ ) of 2.4 eV, a coupling constant ( $H_{AB}$ ) of 0.9 cm<sup>-1</sup>, a free energy change ( $\Delta G^\circ$ ) of -22.0 kJ/mol, and a donor–acceptor distance ( $r$ ) of 14 Å. These values are consistent with parameters deduced for electron transfer reactions in other protein–protein systems where electron transfer is rate-limiting. Finally, the electron transfer reaction within the L127Δ Fe protein–MoFe protein complex was found to be reversible. These results are discussed in the context of models for how MgATP interactions might be coupled to electron transfer in nitrogenase.

Nitrogenase-catalyzed substrate reduction reactions require electron transfer from the iron (Fe) protein<sup>1</sup> component to the molybdenum–iron (MoFe) protein component in a reaction that is coupled to the hydrolysis of MgATP (1–6). The flow of electrons proceeds from a [4Fe-4S] cluster in the Fe protein to a P-cluster (or [8Fe-7S]) (7, 8) in the MoFe protein (9) and finally to an iron–molybdenum–sulfur–homocitrate cofactor (FeMoco) (10), the site of substrate binding and reduction (11, 12). MgATP appears to serve at least three important functions in this overall reaction, namely, (i) the binding of MgATP to the Fe protein component of nitrogenase induces protein conformational

changes (6) that are a prerequisite for the proper docking of this protein to the MoFe protein, (ii) the hydrolysis of MgATP by the Fe protein–MoFe protein complex is coupled by an unknown mechanism to the transfer of an electron from the Fe protein to the MoFe protein (1), and finally (iii) the hydrolysis of MgATP to MgADP appears to be involved in triggering dissociation of the Fe protein from the MoFe protein following electron transfer (13–18). Thus, nitrogenase appears to provide a unique case of biological electron transfer that is coupled to MgATP hydrolysis. Interestingly, from an X-ray crystal structure of a nitrogenase Fe protein–MoFe protein complex, it is known that the two MgATP binding sites on the Fe protein are at least 15 Å away from the metal centers involved in electron transfer (19). This architecture demands that nucleotides must exert their effects on electron transfer through long-range protein conformational changes (4).

The kinetics of electron transfer reactions within nitrogenase have been extensively investigated (17, 18, 20, 21). Despite these studies, there is still considerable debate about the details of how these two different reactions are coupled. It is apparent that MgATP hydrolysis dramatically influences the rate of electron transfer between the two nitrogenase

<sup>†</sup> This work was supported by National Science Foundation Grants MCB-9722937 (L.C.S.) and CHE-9708935 (V.D.P.).

\* Address correspondence to this author. Phone: (801) 797-3964. Fax: (801) 797-3390. E-mail: seefeldt@cc.usu.edu.

<sup>⊗</sup> Abstract published in *Advance ACS Abstracts*, December 1, 1997.

<sup>1</sup> Abbreviations: Fe protein, iron protein of nitrogenase; MoFe protein, molybdenum–iron protein of nitrogenase; HEPES, 4-(2-hydroxyethyl)-1-piperazineethanesulfonic acid;  $E_m$ , midpoint potential;  $\Delta S^\ddagger$ , activation entropy;  $\Delta H^\ddagger$ , activation enthalpy;  $\lambda$ , reorganization energy;  $H_{AB}$ , electronic coupling;  $r$ , distance between redox donor and acceptor;  $\beta$ , electron pathway medium constant; L127Δ, altered form of the Fe protein with Leu at position 127 deleted;  $k$ , rate constant;  $K$ , equilibrium constant.

component proteins (14), and may play a possible role in reducing substrates. At a minimum, two MgATP molecules must be hydrolyzed for each electron transferred between the two nitrogenase proteins (21), but how the energy of the hydrolysis reaction is coupled to electron transfer is not well understood.

Recently, we discovered that removal of a single amino acid within the Fe protein significantly changes the coupling between MgATP hydrolysis and electron transfer (14). A Leu residue at position 127 in the Fe protein from *Azotobacter vinelandii* is located in what appears to be a communication pathway from the nucleotide binding site to the [4Fe-4S] cluster (1, 4). Deletion of this residue results in a protein that appears to be in a conformation resembling the MgATP-bound state even in the absence of bound nucleotides (22). While the L127Δ Fe protein will not support substrate reduction when combined with the MoFe protein, it was found to form a tight complex with the MoFe protein even in the absence of MgATP (14). This irreversible protein–protein complex is in contrast to the wild-type Fe protein–MoFe protein complex, which is only transiently formed during turnover. Surprisingly, it was found that the L127Δ Fe protein variant transferred a single electron to the MoFe protein in the absence of MgATP hydrolysis (14). The L127Δ Fe protein was not able to transfer a second electron (a minimum of two electrons are required to reduce the simplest substrates), probably since the two proteins could not dissociate, explaining the lack of substrate reduction. Thus, unlike the wild-type nitrogenase complex, MgATP hydrolysis is not absolutely required for primary electron transfer in the L127Δ variant. The availability of these two different nitrogenase complexes, namely, the MgATP-dependent wild-type case and the MgATP-independent L127Δ variant, provides a unique opportunity to examine the role of MgATP hydrolysis in the nitrogenase electron transfer reaction.

Electron transfer (Marcus) theory (23) provides a quantitative way to describe electron transfer reactions and has been applied to several biological electron transfer systems (24–27). In this theory, the rate of electron transfer ( $k_{ET}$ ) is related to the temperature of the reaction by a series of parameters according to eqs 1 and 2:

$$k_{ET} = \frac{4\pi^2(H_{AB})^2}{h\sqrt{4\pi\lambda RT}} e^{[-(\Delta G^\circ + \lambda)^2]/4\lambda RT} \quad (1)$$

$$k_{ET} = k_0 e^{-\beta(r-r_0)} e^{[-(\Delta G^\circ + \lambda)^2]/4\lambda RT} \quad (2)$$

where  $h$  is Planck's constant,  $R$  is the gas constant,  $k_0$  is the characteristic frequency of the nuclei (assigned a value of  $10^{13} \text{ s}^{-1}$ ), and  $r_0$  is the close contact distance (assigned a value of 3 Å). The Marcus parameters that describe electron transfer are as follows: (i)  $H_{AB}$ , the coupling constant, a measure of the degree of wave function overlap between the electron acceptor and the donor; (ii)  $\lambda$ , the reorganizational energy; (iii)  $\beta$ , the electronic decay factor, which is related to the nature of the intervening medium between the electron acceptor and donor; (iv)  $r$ , the interatomic distance between the acceptor and the donor; and (v)  $\Delta G^\circ$ , the standard free energy change for the reaction. By measuring the temperature dependence of electron transfer rates and fitting the

data to eqs 1 and 2, it is possible to derive the above Marcus parameters (27). Comparison of these parameters to values obtained from theoretical and experimental studies on related systems can be used to gain insights into the electron transfer reaction. In particular, the type of electron transfer reaction (true, gated, or coupled) can be determined (27, 28). If the electron transfer reaction is the rate-limiting step, then the reaction can be described as either true or coupled. In true electron transfer, the electron transfer step is rate-limiting. In the coupled reaction, electron transfer is also rate-limiting, but a fast, thermodynamically unfavorable reaction precedes the electron transfer step. In contrast, if an adiabatic event (e.g., a protein conformational change) precedes electron transfer and is rate-limiting to the overall reaction, then the electron transfer reaction is said to be gated (28, 29). In this case, Marcus theory is not applicable as evidenced by inappropriate values of the Marcus parameters (27).

In the present work, we have applied Marcus theory to the two cases of electron transfer in nitrogenase, the MgATP-dependent and MgATP-independent cases, to gain insights into the function of MgATP hydrolysis in the intercomponent electron transfer reaction. Our results provide evidence that events associated with MgATP interaction gate intercomponent electron transfer, and that deletion of the single amino acid, Leu 127, in the Fe protein can convert the nitrogenase reaction to true or coupled electron transfer, where electron transfer is rate-limiting. The Marcus parameters derived for this latter reaction are compared to values seen in other biological electron transfer systems. In addition, evidence is presented that this latter electron transfer reaction is reversible, suggesting a possible role for MgATP hydrolysis in making electron transfer unidirectional.

## EXPERIMENTAL PROCEDURES

**Expression and Purification of Nitrogenase Proteins.** Wild-type nitrogenase Fe and MoFe proteins were expressed in *Azotobacter vinelandii* cells and were purified as previously described (30). The altered Fe protein with Leu at position 127 deleted (L127Δ) was constructed, expressed, and purified as described (22). All proteins were homogeneous as determined by Coomassie staining of SDS gels (31), and the wild-type nitrogenase proteins had specific activities of at least 2000 nmol of acetylene reduced·min<sup>-1</sup>·(mg of protein)<sup>-1</sup> (32). Protein concentrations were determined either by a biuret assay (33) or from the visible absorption coefficients of 13.3 mM<sup>-1</sup>·cm<sup>-1</sup> at 400 nm for the oxidized Fe protein (34), 11.1 mM<sup>-1</sup>·cm<sup>-1</sup> at 400 nm for the reduced Fe protein (35), and 62.3 mM<sup>-1</sup>·cm<sup>-1</sup> at 400 nm for the MoFe protein (36). All manipulations were done in the absence of oxygen inside a glovebox (Coy Products, Grass Lake, MI) with a gas atmosphere of 95% N<sub>2</sub> and 5% H<sub>2</sub> and an oxygen concentration of less than 1 ppm. Unless otherwise noted, all buffer solutions contained 2 mM dithionite (Na<sub>2</sub>S<sub>2</sub>O<sub>4</sub>).

**Kinetic Analysis.** Electron transfer from the nitrogenase Fe protein to the MoFe protein was monitored by the increase in the visible absorbance of the Fe protein upon oxidation of the [4Fe-4S] cluster from the reduced (1+) to the oxidized (2+) oxidation state<sup>2</sup> (37). This electron transfer reaction was monitored in real-time by use of a Hi-Tech SF61

stopped-flow spectrophotometer equipped with a data acquisition and curve-fitting system (Salisbury, Wilts, U.K.). The SHU-61 sample handling unit was kept anoxic inside an anaerobic glovebox operating at less than 1 ppm oxygen. Reactant solutions were thermostated to within  $\pm 0.1$  °C by means of a closed-circulation Techne C-85D water circulator (Techne Ltd., Duxford, Cambridge, U.K.) attached to a FC-200 Techne flow cooler. Both the flow cooler and circulator were external to the anaerobic chamber. Data were collected at 430 nm for the oxidation/reduction of Fe protein (14). Earlier work has demonstrated no significant changes in the absorption coefficient of the MoFe protein at 430 nm resulting from electron transfer from the Fe protein (37). All reactions were carried out in 100 mM HEPES buffer, pH 7.4, with 2 mM dithionite. In all cases, reactions were initiated by rapidly mixing reactants contained in the two drive syringes of the stopped-flow instrument. The instrument mixing time was determined to be approximately 4 ms. Reaction conditions are noted in the appropriate figure legends.

Apparent first-order rate constants for electron transfer ( $k_{\text{obs}}$ ) were determined from nonlinear, least-squares fits of the absorbance versus time traces to the equation for a single exponential. In all cases, the absorbance versus time traces represented the average of three consecutive experiments.

**Marcus Analysis.** The Marcus parameters for the nitrogenase electron transfer reactions were determined from the temperature dependence of the apparent electron transfer rate constants ( $k_{\text{obs}}$ ). These data were fit to eqs 1 and 2, which describe nonadiabatic electron transfer reactions derived using Marcus theory (23, 27). The data were first fit to eq 1 using a nonlinear least-squares method in the program Igor Pro (Wavemetrics, Lake Oswego, OR) to obtain (i)  $H_{\text{AB}}$ , the electronic coupling between the electron acceptor and the donor, (ii)  $\lambda$ , the reorganization energy, and (iii)  $\Delta G^\circ$ , the standard free energy difference for the reaction. The gas constant ( $R$ ) was taken as 8.314 J/(K·mol), Planck's constant ( $h$ ) as  $6.626 \times 10^{-34}$  J·s, and the temperature ( $T$ ) in kelvin. Using the values of  $\Delta G^\circ$  and  $\lambda$  obtained from fitting the data to eq 1, the data were then fit to eq 2 to obtain (i)  $r$ , the distance between electron donor and acceptor, and (ii)  $\beta$ , the electronic decay factor, which is related to the nature of the intervening medium between the electron acceptor and donor (38, 39). The characteristic frequency of the nuclei ( $k_o$ ) was assigned a value of  $10^{13}$  s $^{-1}$ , and the close contact distance ( $r_o$ ) was assigned a value of 3 Å (26).

**Activation Parameters.** For the application of transition state theory, plots of the ln of the observed rate constants ( $k_{\text{obs}}$ ) versus  $1/T$  were fit to eq 3, where  $h$  is Planck's constant,  $R$  is the gas constant,  $T$  is the absolute temperature, and  $k_B$  is Boltzmann's constant ( $1.380 \times 10^{-23}$  J/K).

$$\ln\left(\frac{k_{\text{obs}}h}{k_B T}\right) = \frac{-\Delta H^\ddagger}{RT} + \frac{\Delta S^\ddagger}{R} \quad (3)$$

The activation enthalpy ( $\Delta H^\ddagger$ ) and the activation entropy ( $\Delta S^\ddagger$ ) for the reaction were obtained from fits of the data to eq 3.

<sup>2</sup> The redox couples of low potential [4Fe-4S] clusters can also be defined in terms of the formal charges of the entire cluster [4Fe-4S(Cys)<sub>4</sub>] where the 2+/1+ couple is defined as 2-/3-.

**Equilibrium Electron Transfer between the L127Δ Fe Protein and the MoFe Protein.** The electron transfer equilibrium constant for the reaction between the L127Δ Fe protein and the MoFe protein was determined from the ratio of oxidized to reduced L127Δ Fe protein ( $[4\text{Fe-4S}]^{2+}/[4\text{Fe-4S}]^{1+}$ ) following electron transfer. This was conveniently determined from the final absorbance value reached at long times in the stopped-flow experiment. Electron transfer reactions were conducted by mixing reduced L127Δ Fe protein in one syringe with MoFe protein in the other syringe and allowing the reaction to proceed to completion at defined temperatures. The final absorbance value for indigodisulfonate-oxidized L127Δ Fe protein alone was taken to be 100% oxidized, and the absorbance value for the dithionite-reduced L127Δ Fe protein alone was taken to be 100% reduced. For absorbance values between these two extremes, it was possible to establish the ratio of oxidized to reduced  $[4\text{Fe-4S}]^{2+/1+}$  cluster. The equilibrium constant ( $K_{\text{ET}}$ ) for the reversible electron transfer reaction was taken as the ratio of the concentration of the oxidized to reduced L127Δ Fe protein at equilibrium. The other thermodynamic parameters were calculated from the standard thermodynamic relationships in eq 4:

$$\Delta G^\circ = -RT \ln(K_{\text{ET}}) = -nF\Delta E_m = \Delta H^\circ - T\Delta S^\circ \quad (4)$$

where  $\Delta E_m$  is the difference in midpoint potential,  $\Delta G^\circ$  is the standard Gibbs free energy change,  $\Delta H^\circ$  is the standard enthalpy change,  $\Delta S^\circ$  is the standard entropy change,  $R$  is the gas constant, and  $F$  is the Faraday constant [96 495 J/(V·mol)].

**Freeze-Quench EPR Spectroscopy.** The electron transfer equilibrium between the L127Δ Fe protein and the MoFe protein was trapped by rapid freezing of samples poised at different equilibrium temperature conditions. The success of this experiment depended on the fact that the rate constant for establishing equilibrium was much slower than the rate of freezing of the samples. In the experiment, a solution containing L127Δ Fe protein (142 μM) and MoFe protein (75 μM) in 50 mM HEPES buffer, pH 7.4, was allowed to react to completion at 25 °C for 1 h. The sample was split into four equal fractions and then incubated an additional 1 h at either 5, 10, 16, or 25 °C. The samples were then rapidly frozen in EPR tubes by plunging the tubes into a hexane-liquid nitrogen slurry. EPR spectra were recorded on a Bruker ESP300E spectrometer equipped with a dual-mode cavity and an Oxford ESR 900 liquid helium cryostat. In all cases, 4 mm calibrated quartz EPR tubes (Wilma, Buena, NJ) were used. All EPR spectra were recorded at 12 K, with a microwave power of 1.01 mW, a microwave frequency of 9.64 GHz, a modulation frequency of 100 kHz, a modulation amplitude of 5.028 G, a conversion time of 10.24 ms, and a time constant of 10.24 ms. Each spectrum was the sum of 10 scans.

## RESULTS

**Temperature Dependence of Primary Electron Transfer in Nitrogenase.** Electron transfer from the nitrogenase Fe protein to the MoFe protein can be followed by a change in absorption at 430 nm resulting from the difference in the absorption coefficients between the oxidized  $[4\text{Fe-4S}]^{2+}$  cluster and the reduced  $[4\text{Fe-4S}]^{1+}$  cluster of the Fe protein

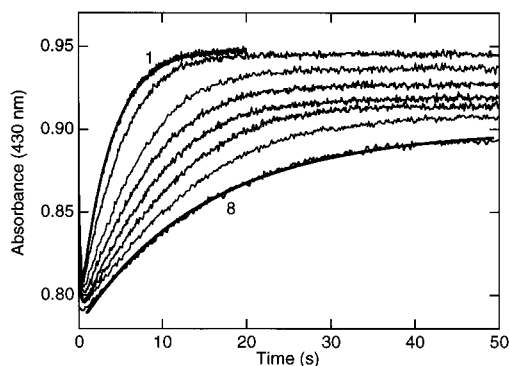
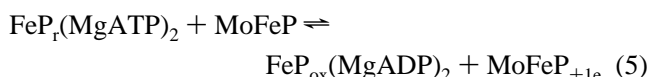


FIGURE 1: Temperature dependence of primary electron transfer rates from the L127 $\Delta$  Fe protein to the MoFe protein. Reduced L127 $\Delta$  Fe protein and MoFe protein samples were prepared as described under Experimental Procedures. Electron transfer was monitored by following the oxidation of the L127 $\Delta$  Fe protein [4Fe-4S] cluster from the 1+ to the 2+ oxidation states by stopped-flow absorption spectroscopy at 430 nm. Absorbance traces are shown after mixing L127 $\Delta$  Fe protein (75  $\mu$ M) contained in one syringe with MoFe protein (20  $\mu$ M) contained in the second syringe. The experimental temperatures were: trace 1 = 30.9  $^{\circ}$ C, trace 2 = 25.8  $^{\circ}$ C, trace 3 = 20.1  $^{\circ}$ C, trace 4 = 17.9  $^{\circ}$ C, trace 5 = 16.1  $^{\circ}$ C, trace 6 = 14.2  $^{\circ}$ C, trace 7 = 12.4  $^{\circ}$ C, and trace 8 = 11.0  $^{\circ}$ C. The heavy solid lines on top of traces 1 and 8 are fits of the data to the equation for a single exponential.

(37). No significant changes in absorption coefficient have been observed for the MoFe protein upon reduction by the Fe protein. Using stopped-flow absorption spectroscopy, it is therefore possible to monitor the primary electron transfer reaction from the Fe protein to the MoFe protein (eq 5) by following the increase in absorption at 430 nm resulting from the oxidation of the [4Fe-4S] cluster (37).



The kinetics of the reaction are pseudo-first-order under the reaction conditions used in this work and thus can be fit to a single exponential equation to obtain pseudo-first-order rate constants for the observed electron transfer reaction ( $k_{\text{obs}}$ ). For the wild-type nitrogenase primary electron transfer reaction at 23  $^{\circ}$ C, an observed rate constant of 150  $\text{s}^{-1}$  was determined, which is consistent with values reported earlier for this reaction (6). This electron transfer reaction was also found to be temperature dependent, with slower rates observed at lower temperatures, consistent with earlier work (40). This indicates a nonzero activation enthalpy ( $\Delta H^{\ddagger}$ ) for the electron transfer reaction. Similarly, the MgATP-independent electron transfer reaction from the L127 $\Delta$  Fe protein to the MoFe protein is observed to be pseudo-first-order under these conditions with a temperature dependence on the rate of reaction (Figure 1). It is noteworthy that the rate of electron transfer for the MgATP-independent reaction ( $k_{\text{obs}} = 0.18 \text{ s}^{-1}$  at 23  $^{\circ}$ C) is approximately 1000-fold slower than that observed for the MgATP-dependent wild-type nitrogenase reaction.

The observed rate constants ( $k_{\text{obs}}$ ) measured at different temperatures for the two reaction types are plotted against the temperature of the reaction in Figure 2. Fits of these data to the Marcus equations (eqs 1 and 2) are shown as the two solid lines in Figure 2. The data were first fit to equation 1 with the unknown variables being  $\Delta G'^{\circ}$ ,  $H_{\text{AB}}$ , and  $\lambda$ . All

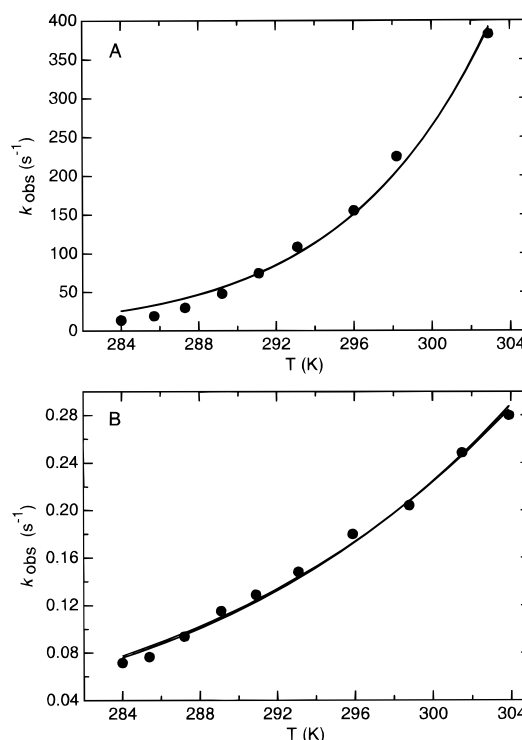


FIGURE 2: Marcus analysis of the temperature dependence of the observed electron transfer rate constants ( $k_{\text{obs}}$ ). The observed rate constants for electron transfer ( $k_{\text{obs}}$ ) from the nitrogenase Fe protein to the MoFe protein were plotted against the experimental temperatures for electron transfer in the MgATP-dependent reaction from the wild-type Fe protein to the MoFe protein (panel A) or in the MgATP-independent electron transfer reaction from the L127 $\Delta$  Fe protein to the MoFe protein (panel B). The solid lines represent nonlinear, least-squares fits of the data to eqs 1 and 2 described in the text. The Marcus parameters derived from these fits are summarized in Table 1. Each point is the average observed rate constant from three separate reactions, where the standard deviation between the observed values was less than 2.1%.

other parameters were held constant as specified under Experimental Procedures. The values for  $H_{\text{AB}}$ ,  $\lambda$ , and  $\Delta G'^{\circ}$  obtained from these fits are tabulated in Table 1. Using the values of  $\Delta G'^{\circ}$  and  $\lambda$  obtained from the fit to eq 1, the temperature-dependent rate data were then fit to the second Marcus equation (eq 2), resulting in the second solid line in Figure 2. From this fit, the values of  $r$ , the distance between the electron acceptor and donor, and  $\beta$ , the electronic decay factor, were determined (Table 1). A comparison of the Marcus parameters (Table 1) derived for the MgATP-dependent electron transfer reaction in wild-type nitrogenase and the MgATP-independent electron transfer in the L127 $\Delta$  Fe protein–MoFe protein complex to theoretically and experimentally determined values from other systems provides an indication of the relevance of Marcus theory to these two cases (27). Several of the Marcus parameters (e.g.,  $H_{\text{AB}}$ ,  $r$ ,  $\beta$ ) derived for wild-type nitrogenase electron transfer are unreasonable and thus indicate that Marcus theory is not applicable. This suggests an adiabatic event (e.g., a conformational change) is preceding the electron transfer reaction and contributes to the rate of the reaction.

In contrast, the thermodynamic parameters derived for the MgATP-independent electron transfer reaction from the L127 $\Delta$  Fe protein to the MoFe protein are consistent with accepted values for these parameters (27), suggesting the applicability of Marcus theory. Most telling of these

Table 1: Activation and Marcus Parameters for Electron Transfer from the Wild-Type and L127Δ Iron Proteins to the Molybdenum–Iron Protein

parameter <sup>a</sup>	iron protein	
	wild-type	L127Δ
$\Delta S^\ddagger$ (J·mol <sup>-1</sup> ·K <sup>-1</sup> )	+125 <sup>b</sup> +360	−100
$\Delta H^\ddagger$ (kJ·mol <sup>-1</sup> )	+97 +165	+46
$\lambda$ (eV)	[4.42] <sup>c</sup>	2.4 ± 0.3 <sup>d</sup>
$H_{AB}$ (cm <sup>-1</sup> )	[7.42 × 10 <sup>12</sup> ]	0.9 ± 0.4
$\Delta G'^\circ$ (kJ·mol <sup>-1</sup> )	[−5.8]	−22.0 ± 2.5
$r$ (Å)	[−84]	14 ± 1.5
$\beta$ (Å <sup>-1</sup> )	[0.19]	1.1 ± 0.2

<sup>a</sup> The activation parameters  $\Delta S^\ddagger$  and  $\Delta H^\ddagger$  were determined from fits of the data in Figure 3 to eq 3, with the error in the reported values being less than 5%. The Marcus parameters  $\lambda$ ,  $H_{AB}$ , and  $\Delta G'^\circ$  were determined from fits of the data in Figure 2 to eq 1. The Marcus parameters  $r$  and  $\beta$  were determined from fits of the data in Figure 2 to eq 2 using the values for  $\lambda$ ,  $H_{AB}$ , and  $\Delta G'^\circ$  obtained from the first fit. <sup>b</sup> The first numbers for the wild-type nitrogenase reaction are for the temperature range from 291 to 304 K, and the second numbers are for the temperature range from 284 to 291 K. For the L127Δ Fe protein–MoFe protein complex, the reported values are from a fit of the data in Figure 2 to eq 3 over the entire temperature range. <sup>c</sup> The brackets indicate that these parameters are not physically meaningful because the formalism used to analyze the data may be inappropriate. <sup>d</sup> The reported errors represent the standard deviation from three independent experiments.

parameters is the value of  $r$ , the measure of the interatomic distance between the electron acceptor and the electron donor. A value of 14 Å is calculated from the Marcus equation (eq 2) for the L127Δ Fe protein–MoFe protein reaction, which is identical to the distance between the [4Fe-4S] cluster of the Fe protein and a P-cluster of the MoFe protein within a nitrogenase complex (19). The uniqueness of the values obtained for the Marcus parameters presented in Table 1 was accessed by fitting the data in Figure 2 to eqs 1 and 2, holding the value of  $r$  constant at values other than 14 Å. From such an analysis, it was possible to obtain reasonable values for  $\beta$ ,  $\lambda$ , and  $\Delta G'^\circ$  when the value of  $r$  ranged from 13 to 16 Å. Values of  $r$  outside of this range resulted in poor fits to the data. In summary, a single amino acid alteration within the Fe protein appears to have changed the mechanism of electron transfer so that electron transfer has become rate-limiting.

**Application of Transition State Theory.** The unreasonable values of Marcus parameters for the MgATP-dependent electron transfer reaction in wild-type nitrogenase suggest that an adiabatic event is contributing to the reaction rate and thus that transition state theory is more appropriate to analyze this reaction. Figure 3 (panel B) shows an Arrhenius plot of the ln of the observed rate constants ( $k_{\text{obs}}$ ) versus  $1/T$  for the wild-type reaction. Interestingly, a break in the plot is observed, indicating a change in the rate-limiting step of the reaction over this temperature range. The activation parameters derived for the two different temperature ranges are tabulated in Table 1. These results are similar to results previously reported for this reaction (40). Over the temperature range from 291 to 304 K, the values obtained for  $\Delta H^\ddagger$  and  $\Delta S^\ddagger$  were +97 kJ/mol and +125 J/(mol·K), similar to the previously published values of +90 kJ/mol and +99 J/(mol·K) (40). The values of  $\Delta H^\ddagger$  and  $\Delta S^\ddagger$  obtained over the temperature range from 284 to 291 K were +165 kJ/

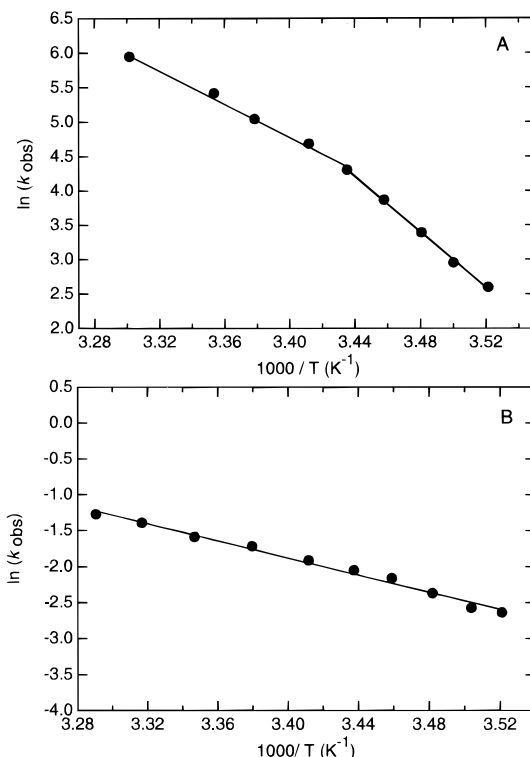


FIGURE 3: Thermodynamic analysis of the electron transfer reactions from the Fe protein to the MoFe protein. The natural logarithms of the observed rate constants ( $k_{\text{obs}}$ ) for electron transfer from the Fe protein to the MoFe protein were plotted against  $1/\text{temperature}$  for the MgATP-dependent electron transfer from the wild-type Fe protein to the MoFe protein (panel A) or for the MgATP-independent electron transfer from the L127Δ Fe protein to the MoFe protein (panel B). The solid lines represent linear fits to the Eyring equation (eq 3). The derived thermodynamic parameters of activation are presented in Table 1.

mol and +360 J/(mol·K), again were similar to values reported over this temperature range (40). Thus, the rate-limiting step(s) in the wild-type nitrogenase electron transfer reaction represent(s) a highly disordered state, with an unfavorable change in the enthalpy of activation.

In contrast to the wild-type nitrogenase reaction, the Arrhenius plot for the MgATP-independent L127Δ Fe protein–MoFe protein electron transfer reaction is linear over the temperature range from 284 to 303 K, indicating that the events contributing to the transition state do not change. This is consistent with the results from Marcus analysis, suggesting that electron transfer is rate-limiting. Interestingly, while the activation enthalpy ( $\Delta H^\ddagger$ ) for the reaction is similar to that observed for the MgATP-dependent reaction in wild-type nitrogenase, the activation entropy ( $\Delta S^\ddagger$ ) is dramatically different, being of opposite sign (Table 1). Negative values of the activation entropy have been observed for other protein–protein electron transfer reactions, although the meaning of these values is not clear (41, 42).

**Electron Transfer Equilibrium.** An interesting observation from the stopped-flow traces of nitrogenase electron transfer is that the final equilibrium absorbance value is also temperature dependent (Figure 1). This observation indicates that the ratio of oxidized to reduced [4Fe-4S] cluster is changing with temperature, suggesting that the electron transfer reaction is reversible, with a temperature-dependent equilibrium constant. While similar results have been interpreted in the past as indicating reversibility of electron

Table 2: Thermodynamic Parameters for the Electron Transfer Equilibrium in the Nitrogenase L127Δ Fe Protein–MoFe Protein Complex

temperature (°C)	$K_{ET}^a$	$\Delta G'^{\circ}$ (kJ·mol <sup>-1</sup> )	$\Delta E_m$ (mV)
11.1	1.4 ± 0.3	-0.8	8
12.5	1.9 ± 0.7	-1.5	16
13.5	3.8 ± 0.9	-3.2	33
16.3	7.0 ± 1.1	-4.6	47
19.2	13.0 ± 5.0	-6.3	65
22.0	69.0 ± 10.4	-10.4	107

<sup>a</sup> Values for  $K_{ET}$  were determined from the ratio of oxidized/reduced Fe protein calculated from the final equilibrium absorbance values in stopped-flow experiments similar to that shown in Figure 1. The uncertainty reported represents the standard deviation from six independent measurements.

transfer in wild-type nitrogenase (43), these interpretations are complicated by the continuous hydrolysis of MgATP. The electron transfer reaction in the L127Δ Fe protein–MoFe protein complex occurs without MgATP hydrolysis. This makes interpretation of the temperature dependence of the electron transfer equilibrium tractable. Figure 1 demonstrates that the final equilibrium absorbance value for the L127Δ Fe protein–MoFe protein reaction was temperature dependent, indicating reversible electron transfer. The reversibility of this reaction was confirmed by cycling the temperature and observing that the final absorbance value returned to the starting absorbance value. Using the final equilibrium absorbance value at different temperatures, it was possible to calculate the ratio of oxidized to reduced [4Fe-4S] cluster at each reaction temperature. From this ratio, the electron transfer equilibrium constant ( $K_{ET}$ ) was calculated, along with the free energy change ( $\Delta G'^{\circ}$ ) and midpoint potential difference ( $\Delta E_m$ ) at each reaction temperature. As can be seen from the data in Table 2, the midpoint potential difference between the electron donor and electron acceptor (presumably the [4Fe-4S] cluster and P-cluster) changes from 8 mV to over 100 mV over a 11 °C temperature range.

Freeze-quench EPR studies were employed to confirm that the changes in the final absorption values from the stopped-flow experiments were the result of changes in the oxidation state of the [4Fe-4S] cluster. It is possible that the changes in the absorption values at 430 nm are not simply reporting the changes in oxidation state of the [4Fe-4S] cluster, but might be complicated by other events such as a change in the absorption maximum of the [4Fe-4S] cluster in the complex (18) or by changes in the absorption coefficient of metal centers in the MoFe protein. EPR provides a method to quantify the oxidation state of the [4Fe-4S] cluster without interference from the other metal centers. In this experiment, the L127Δ Fe protein–MoFe protein complex was allowed to incubate at a defined temperature for 1 h to allow the electron transfer reaction to reach equilibrium. The sample was then rapidly frozen by plunging the EPR tube containing the sample into a slurry of hexane and liquid nitrogen. This results in the rapid freezing of the sample (less than 1 s). This experiment was dependent on the relatively slow change in the electron transfer equilibrium with changes in temperature and thus allowed the equilibrium to be trapped by freezing the sample before the cooling could change the equilibrium. Figure 4 shows EPR spectra for samples of L127Δ Fe protein–MoFe protein that were rapidly frozen following incubation at various

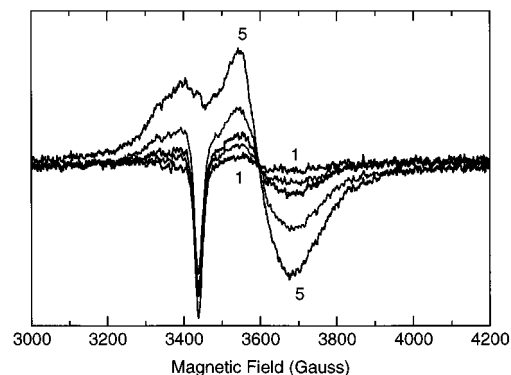


FIGURE 4: Freeze-quench of the electron transfer equilibrium between the L127Δ Fe protein and the MoFe protein. Electron transfer between the L127Δ Fe protein (142 μM) and MoFe protein (75 μM) was allowed to reach equilibrium at 25 °C with a 1 h incubation. An aliquot of the sample at 25 °C (trace 1) was placed into an EPR tube and was rapidly frozen as described under Experimental Procedures. The remaining solution was separated into three aliquots, with one aliquot being incubated at 16 °C (trace 2), one at 10 °C (trace 3), and one at 5 °C (trace 4) for 1 h prior to being rapidly frozen in EPR tubes. L127Δ Fe protein alone was incubated for 1 h at 25 °C prior to being frozen in an EPR tube (trace 5). EPR spectra for each sample were recorded as described under Experimental Procedures.

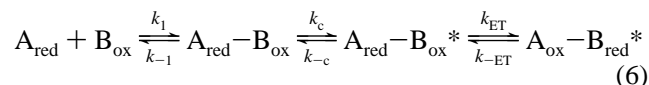
temperatures. From the intensity of the  $g = 1.94$  (3600 Gauss) based signal, it was possible to estimate the ratio of reduced to oxidized [4Fe-4S] cluster at each incubation temperature. From this ratio, the  $K_{ET}$  for each incubation temperature could be determined, and was found to give similar values to those derived from the stopped-flow experiments (Table 2). This confirmed the validity of the analysis of the stopped-flow experiments. These results indicate that the electron transfer reaction in the L127Δ Fe protein–MoFe protein complex is reversible. Furthermore, these results indicate that the electron transferred from the L127Δ Fe protein resides somewhere in the MoFe protein and has not been transferred to the solvent. The location of the electron within the MoFe protein is not clear from the EPR spectra since few changes are apparent in the EPR signals. A slight decrease in the intensity of the EPR signal attributed to FeMoco appears to correlate with the transfer of the electron from the L127Δ Fe protein, which has been suggested to indicate that the electron may partially reside at FeMoco (14).

## DISCUSSION

The application of Marcus theory to the two different nitrogenase intercomponent electron transfer reactions investigated in the present study provides insights into how MgATP interactions are coupled to electron transfer. The results of the present work are discussed in the broader context of protein–protein electron transfer, along with the implications for understanding the mechanisms for coupling these two diverse reactions in nitrogenase.

**Nitrogenase Electron Transfer Reactions.** Marcus analysis highlights the fundamental differences between the mechanism of the electron transfer reaction for the wild-type Fe protein–MoFe protein nitrogenase complex and for the L127Δ Fe protein–MoFe protein nitrogenase complex. In the wild-type nitrogenase electron transfer reaction, which absolutely requires MgATP interactions, the Marcus param-

eters were found to be significantly outside of the values expected from both theoretical and experimental studies (27). In the Marcus formalism (23), the electron transfer reaction is assumed to be a nonadiabatic reaction. From calculations of the dynamic relaxation rates of water, a maximum value for the coupling constant ( $H_{AB}$ ) of  $80 \text{ cm}^{-1}$  is predicted (24). The value of  $H_{AB}$  obtained for the MgATP-dependent electron transfer reaction within the wild-type nitrogenase was  $7.42 \times 10^{12} \text{ cm}^{-1}$ . Clearly this value is significantly larger than the theoretical maximum value, indicating that electron transfer is not rate-limiting, but rather that some adiabatic reaction is contributing to the electron transfer reaction. This is also evident from the unreasonable value obtained for the electronic decay factor ( $\beta$ ) of  $0.19 \text{ \AA}^{-1}$ . Both theoretical and experimental studies (44) suggest a range for  $\beta$  of  $0.7\text{--}1.4 \text{ \AA}^{-1}$  for proteins. Likewise, the value obtained for the reorganizational energy ( $\lambda$ ) of  $4.42 \text{ eV}$  is significantly larger than the values obtained in other protein electron transfer reactions of about  $2.5 \text{ eV}$  (27, 45). Finally, the most obvious deviation from Marcus theory comes from the value of  $r$ , the interatomic distance between the electron acceptor and the electron donor. For the wild-type nitrogenase reaction, a value of  $-84 \text{ \AA}$  is obtained for  $r$ . A negative number for the interatomic distance is clearly not possible, confirming that electron transfer in wild-type nitrogenase does not conform to Marcus theory. Thus, it must be concluded that some event preceding electron transfer in wild-type nitrogenase is contributing to the electron transfer rate. This can be viewed as the addition of an adiabatic reaction (e.g., a conformational change) which precedes the electron transfer reaction (ET) as shown in eq 6.



The initial docking of the Fe protein ( $A_{\text{red}}$ ) with the MoFe protein ( $B_{\text{ox}}$ ) can be described by the equilibrium constant  $K_1 = k_1/k_{-1}$ . Earlier kinetic studies indicate that  $K_1$  and  $k_1$  are both large (6), and thus this reaction will not contribute to the observed rate of electron transfer. Following docking, it is expected that conformational changes (probably a series of changes) occur before the electron transfer event (18) which can be characterized by the equilibrium constant  $K_c = k_c/k_{-c}$ . This adiabatic step is rate-limiting, explaining why the Marcus formalism is not applicable. Such a reaction sequence has been referred to as gated electron transfer, indicating that an adiabatic reaction gates the electron transfer reaction (27–29).

Evidence that the gating reactions for electron transfer in nitrogenase are associated with MgATP interactions comes from several observations. For the wild-type nitrogenase system, MgATP must be present to allow intercomponent electron transfer. Earlier kinetic studies indicated that the rate constant for electron transfer ( $k_{ET}$ ) was significantly greater than the rate constant for MgATP hydrolysis (18). Thus, it was concluded that MgATP binding, but not hydrolysis, preceded electron transfer, and that MgATP hydrolysis to MgADP and  $P_i$  followed the electron transfer reaction (18). Attainment of the MgADP-bound state of the Fe protein appears to be necessary to allow dissociation of the oxidized Fe protein from the MoFe protein (13–16). The recent discovery that the L127Δ Fe protein variant is able

to transfer a single electron to the MoFe protein in the absence of any MgATP lends support to this proposed sequence of events (14). In this case, a single amino acid deletion in the Fe protein resulted in protein conformational changes, some of which appear to mimic those normally induced by MgATP binding (22). Thus, it would appear that deletion of Leu 127 results in some or all of the conformational changes ( $K_c$ ) normally associated with MgATP binding. Support for this hypothesis comes from the Marcus analysis of the MgATP-independent electron transfer reaction done in the present work. In contrast to the wild-type electron transfer reaction, the L127Δ Fe protein–MoFe protein electron transfer reaction does conform to Marcus theory. Values obtained for  $\lambda$ ,  $H_{AB}$ , and  $\beta$  are consistent with expected values for these parameters in biological electron transfer reactions (27). Most importantly, the value obtained for  $r$ , the interatomic distance between the electron acceptor and donor, of  $14 \text{ \AA}$  is the distance between the Fe protein [4Fe–4S] cluster and the MoFe protein P-cluster within a nitrogenase complex (19). Mounting evidence suggests that a P-cluster is the initial electron acceptor from the [4Fe–4S] cluster (9, 46, 47), making these clusters the likely electron acceptor and donor pair. The apparent applicability of Marcus theory to the electron transfer reaction in the L127Δ Fe protein–MoFe protein complex suggests that electron transfer is rate-limiting in this reaction. Thus, by changing a single amino acid in the Fe protein, the mechanism of the electron transfer reaction has been fundamentally changed such that electron transfer has now become rate-limiting.

Protein electron transfer reactions in which electron transfer is rate-limiting have been referred to as true or coupled reactions (24, 27). True electron transfer would imply that no adiabatic reactions precede electron transfer, and thus only the nonadiabatic electron transfer event is rate-limiting. The other possible mechanism, called coupled electron transfer, holds that an adiabatic reaction precedes electron transfer, but that electron transfer ( $k_{ET}[A_{\text{red}}-B_{\text{ox}}^*]$ ) is rate-limiting, and the equilibrium constant  $K_c$  is small and thus the observed rate constant ( $k_{\text{obs}}$ ) is the product of  $k_{ET}$  and  $K_c$ . With the present data, it is difficult to distinguish between these two mechanisms for the L127Δ Fe protein nitrogenase complex electron transfer reaction. However, one observation may suggest that the reaction mechanism may be better described as coupled. The value of  $2.4 \text{ eV}$  for  $\lambda$ , the reorganization energy, determined for the L127Δ Fe protein nitrogenase complex reaction is relatively large compared to simpler protein electron transfer cases examined which have been described as true electron transfer (24). This suggests that the observed reorganization energy for the L127Δ Fe protein nitrogenase complex contains contributions from both the electron transfer event and preceding adiabatic steps (27). Similar “high” values for the reorganization energy have been observed in other protein–protein electron transfer systems (41, 45, 48), suggesting that the complexity of these systems probably involves some adiabatic steps.

*The Roles of MgATP Hydrolysis.* Thus, one conclusion that can be drawn from the current work is that events associated with MgATP binding must precede and contribute to electron transfer in the nitrogenase reaction. It is important to point out here that these results do not provide information about the relative order of MgATP hydrolysis and electron

transfer. The conformational events ( $K_c$ ) preceding electron transfer associated with MgATP interaction may result from either MgATP binding or MgATP hydrolysis.

It is of interest to know how MgATP interaction events might be coupled to electron transfer. The overall architecture of the nitrogenase complex places the bound MgATP at least 15 Å away from the metal centers involved in the electron transfer (19). Thus, this architecture demands that the effects of MgATP interaction must be communicated as protein conformational changes which impact the electron transfer reaction (1, 4). How might this happen? A model that is developing suggests MgATP binding induces a series of protein conformational changes in the Fe protein, which could impact the electron transfer reaction. An X-ray crystal structure of a nitrogenase Fe protein—MoFe protein complex trapped with MgADP—AlF<sub>4</sub><sup>−</sup> appears to mimic some intermediate state in the course of MgATP hydrolysis (15, 16, 19). The structure reveals significant conformational changes in the Fe protein, suggesting that during the course of MgATP binding and subsequent hydrolysis, a dynamic range of protein conformations are accessed, which could impact the rate and/or thermodynamics of electron transfer between the proteins.

How might these MgATP-dictated conformational changes impact the electron transfer reaction? Recently, a high-resolution X-ray crystal structure of the L127Δ Fe protein—MoFe protein complex has been determined (Peters, Lanzilotta, Ryle, Howard, Seefeldt, and Rees, personal communication), allowing a detailed analysis of possible electron transfer pathways between the Fe protein and the MoFe protein. One electron transfer pathway has emerged as the most likely. This pathway would involve a 3.3 Å through-space jump from a sulfur in the [4Fe-4S] cluster to one of two protein chains in the MoFe protein leading directly to a P-cluster cysteinyl ligand. This pathway provides a simple mechanism for how MgATP binding and hydrolysis might regulate the rate of electron transfer. During the course of MgATP binding, the associated changes in the protein conformation could result in slight changes in the proposed electron transfer pathway, particularly in the distance or orientation of the through-space jump. This could dramatically alter the rate of electron transfer between the proteins (49). Thus, as MgATP binds, the electron transfer pathway might be connected momentarily, and as MgATP is hydrolyzed to MgADP + P<sub>i</sub>, the pathway could be disconnected. Such a model would provide a mechanism for how MgATP binding could gate electron transfer and also provides an explanation for how MgATP hydrolysis could prevent reverse electron transfer from the P-cluster back to the [4Fe-4S] cluster by closing the electron transfer gate. Two observations with the L127Δ Fe protein—MoFe protein complex support this notion. First, the rate of electron transfer within the L127Δ Fe protein—MoFe protein complex is 1000-fold slower than is the wild-type Fe protein—MoFe protein electron transfer reaction. This supports the idea that events associated with MgATP hydrolysis could accelerate the electron transfer reaction. This acceleration could be imagined to result either from altering the pathway of electron transfer (as described above) or by altering the driving force for electron transfer. Recent evidence has indicated that both MgATP binding and Fe protein—MoFe protein complex formation contribute to an increased driving

force for electron transfer (50). Second, the observation of reversible electron transfer in the L127Δ Fe protein—MoFe protein complex may suggest that another function of MgATP hydrolysis is to render the electron transfer reaction irreversible. Again, preventing reverse electron transfer could be accomplished either by a change in the electron transfer pathway or by a change in the driving force for electron transfer.

In summary, the results from the current study provide insights into the relationship between MgATP interactions and intercomponent electron transfer in nitrogenase. It appears that MgATP participates in this electron transfer reaction by regulating the reaction by a gating mechanism. Details of this mechanism are expected to be complex and will require additional work to be elucidated.

## ACKNOWLEDGMENT

We thank Professor David Farrelly and Dr. Ernestine Lee for assistance with nonlinear, least-squares fitting of the temperature dependence data and Professor Victor L. Davidson for helpful advice on the application of electron transfer theory. We also thank Jeannine M. Chan, Matthew J. Ryle, and Dr. Jason Christiansen for helpful discussions.

## REFERENCES

- Howard, J. B., and Rees, D. C. (1994) *Annu. Rev. Biochem.* 63, 235–264.
- Mortenson, L. E., Seefeldt, L. C., Morgan, T. V., and Bolin, J. T. (1993) *Adv. Enzymol.* 67, 299–374.
- Peters, J. W., Fisher, K., and Dean, D. R. (1995) *Annu. Rev. Microbiol.* 49, 335–366.
- Seefeldt, L. C., and Dean, D. R. (1997) *Acc. Chem. Res.* 30, 260–266.
- Hageman, R. V., and Burris, R. H. (1978) *Proc. Natl. Acad. Sci. U.S.A.* 75, 2699–2702.
- Burgess, B. K., and Lowe, D. J. (1996) *Chem. Rev.* 96, 2983–3011.
- Kim, J., and Rees, D. C. (1992) *Nature* 360, 553–560.
- Bolin, J. T., Ronco, A. E., Morgan, T. V., Mortenson, L. E., and Xuong, N. H. (1993) *Proc. Natl. Acad. Sci. U.S.A.* 90, 1078–1082.
- Lowe, D. J., Fisher, K., and Thorneley, R. N. F. (1993) *Biochem. J.* 292, 93–98.
- Orme-Johnson, W. H., Hamilton, W. D., Jones, T. L., Tso, M. Y. W., Burris, R. H., Shah, V. K., and Brill, W. J. (1972) *Proc. Natl. Acad. Sci. U.S.A.* 69, 3142–3145.
- Shah, V. K., and Brill, W. J. (1977) *Proc. Natl. Acad. Sci. U.S.A.* 74, 3249–3253.
- Hawkes, T. R., McLean, P. A., and Smith, B. E. (1984) *Biochem. J.* 217, 317–321.
- Lanzilotta, W. N., Fisher, K., and Seefeldt, L. C. (1997) *J. Biol. Chem.* 272, 4157–4165.
- Lanzilotta, W. N., Fisher, K., and Seefeldt, L. C. (1996) *Biochemistry* 35, 7188–7196.
- Renner, K. A., and Howard, J. B. (1996) *Biochemistry* 35, 5353–5358.
- Duyvis, M. G., Wassink, H., and Haaker, H. (1996) *FEBS Lett.* 380, 233–236.
- Lowe, D. J., Ashby, G. A., Brune, M., Knights, H., Webb, M. R., and Thorneley, R. N. F. (1995) in *Nitrogen Fixation: Fundamentals and Applications* (Tikhonovich, I. A., Provorov, N. A., Romanov, V. I., and Newton, W. E., Eds.) pp 103–108, Kluwer Academic, Dordrecht.
- Duyvis, M. G., Wassink, H., and Haaker, H. (1996) *J. Biol. Chem.* 271, 29632–29636.
- Schindelin, H., Kisker, C., Schlessman, J. L., Howard, J. B., and Rees, D. C. (1997) *Nature* 387, 370–376.



20. Thorneley, R. N. F., and Lowe, D. J. (1985) in *Molybdenum Enzymes* (Spiro, T. G., Ed.) pp 221–284, Wiley, New York.
21. Hageman, R. V., Orme-Johnson, W. H., and Burris, R. H. (1980) *Biochemistry* 19, 2333–2342.
22. Ryle, M. J., and Seefeldt, L. C. (1996) *Biochemistry* 35, 4766–4775.
23. Marcus, R. A., and Sutin, N. (1985) *Biochim. Biophys. Acta* 811, 265–322.
24. Winkler, J. R., and Gray, H. B. (1992) *Chem. Rev.* 92, 369–379.
25. McLendon, G. (1988) *Acc. Chem. Res.* 21, 160–167.
26. Rees, D. C., and Farrelly, D. (1990) *Enzymes (3rd Ed.)* 19, 37–97.
27. Davidson, V. L. (1996) *Biochemistry* 35, 14035–14039.
28. Hoffman, B. M., and Ratner, M. A. (1987) *J. Am. Chem. Soc.* 109, 6237–6243.
29. Brunschwig, B. S., and Sutin, N. (1989) *J. Am. Chem. Soc.* 111, 7454–7465.
30. Seefeldt, L. C., and Mortenson, L. E. (1993) *Protein Sci.* 2, 93–102.
31. Hathaway, G. M., Lundak, T. S., Tahara, S. M., and Traugh, J. A. (1979) *Methods Enzymol.* 60, 495–511.
32. Seefeldt, L. C., and Ensign, S. A. (1994) *Anal. Biochem.* 221, 379–386.
33. Chromy, V., Fischer, J., and Kulhanek, V. (1974) *Clin. Chem.* 20, 1362–1363.
34. Lanzilotta, W. N., Ryle, M. J., and Seefeldt, L. C. (1995) *Biochemistry* 34, 10713–10723.
35. Watt, G. D., Wang, Z. C., and Knotts, R. R. (1986) *Biochemistry* 25, 8156–8162.
36. Watt, G. D., and Wang, Z. C. (1989) *Biochemistry* 28, 1844–1850.
37. Thorneley, R. N. F., and Lowe, D. J. (1983) *Biochem. J.* 215, 393–403.
38. Moser, C. C., Keske, J. M., Warncke, K., Farid, R. S., and Dutton, P. L. (1992) *Nature* 355, 796–802.
39. Onuchic, J. N., Beratan, D. N., Winkler, J. R., and Gray, H. B. (1992) *Annu. Rev. Biophys. Biomol. Struct.* 21, 349–377.
40. Mensink, R. E., and Haaker, H. (1992) *Eur. J. Biochem.* 208, 295–299.
41. Bishop, G. R., and Davidson, V. L. (1995) *Biochemistry* 34, 12082–12086.
42. Falzon, L., and Davidson, V. L. (1996) *Biochemistry* 35, 12111–12118.
43. Thorneley, R. N. F., Ashby, G., Howarth, J. V., Millar, N. C., and Gutfreund, H. (1989) *Biochem. J.* 264, 657–661.
44. Langen, R., Colon, J. L., Casimiro, D. R., Karpishin, T. B., Winkler, J. R., and Gray, H. B. (1996) *J. Biol. Inorg. Chem.* 1, 221–225.
45. Ivkovic-Jensen, M. M., and Kostic, N. M. (1997) *Biochemistry* 36, 8135–8144.
46. Peters, J. W., Fisher, K., Newton, W. E., and Dean, D. R. (1995) *J. Biol. Chem.* 270, 27007–27013.
47. Lanzilotta, W. N., and Seefeldt, L. C. (1996) *Biochemistry* 35, 16770–16776.
48. Davidson, V. L., and Jones, L. H. (1996) *Biochemistry* 35, 8120–8125.
49. Mutz, M. W., McLendon, G. L., Wishart, J. F., Gaillard, E. R., and Corin, A. F. (1996) *Proc. Natl. Acad. Sci. U.S.A.* 93, 9521–9526.
50. Lanzilotta, W. N., and Seefeldt, L. C. (1997) *Biochemistry* 36, 12976–12983.

BI971681M